TABLE 1
Participating Laboratories

Laboratory	Code	Specimens analyzed	Scoring method	Instrumentation (magnification)
U.S. FDA-NCTR, Rockville, MD and Jefferson, AR	L1	BM, PB	MeOH-AO	Zeiss Axioskop 50 (×630), Zeiss PlanApomat ×63 oil objective
			FCM	BD-FACSort, BD-FACScan
Litron Laboratories, Rochester, NY	L2	PB	FCM	BD-FACSCalibur
Health Canada, Ottawa, Ontario, Canada	L3	PB	FCM	BD-FACSCalibur
National Institute of Health Sciences, Tokyo, Japan	L4	Coordinated SV-AO laboratories		
Nitto Denko Corporation, Osaka, Japan	L5	PB	SV-AO	Olympus AHBT3-RFC (×600)
An-Pyo Center, Shizuoka, Japan	L6	PB	SV-AO	Olympus BX50-RFL (×800)
Astellas Pharma Inc., Tokyo, Japan	L7	PB	SV-AO	Olympus BH-RFL (×600)
N/A to this study	L8			
Contract testing laboratory 1*	L9	BM, PB	MeOH-AO	Leitz Laborlux 12 (×1000)
Contract testing laboratory 2*	L10	BM	MeOH-AO	Olympus BH2 (×1000)
Contract testing laboratory 3*	L11	BM, PB	MeOH-AO	Zeiss STD 14 (×1000)

Note. Abbreviations: FDA-NCTR = U.S. Food and Drug Administration, National Center of Toxicological Research; BM = bone marrow; PB = peripheral blood; MeOH-AO = acridine orange staining of methanol-fixed smears; FCM = flow cytometry; SV-AO = supravital staining using acridine orange-coated slides; N/A = not applicable. *The three contract testing laboratories are BioReliance, Covance, and SRI International, but their identities as L9, L10, or L11 is confidential.

(RET) and MN-RET scoring. Proficiency was assumed based on the high level of training that has occurred at these laboratories (L1, L2, L3, L5, L6, and L7) and/or the frequency with which they contribute *in vivo* rodent MN data for regulatory submission purposes (L9, L10, and L11). See Table 1 for more detailed information regarding collaborating laboratories.

Data presented herein describe the performance characteristics of the three scoring methods evaluated, address the sensitivity of the rat peripheral blood compartment for detecting genotoxicant-induced micronuclei, and support recommendations concerning the minimum number of rat blood RET that should be evaluated for micronuclei.

MATERIALS AND METHODS

Chemicals and other reagents. Cyclophosphamide (CP) (CAS No. 6055-19-2) was purchased from Sigma, St Louis, MO. Acridine orange (AO)–coated slides used for supravital staining, prepared according to the method of Hayashi *et al.* (1990), were provided by the National Institute of Health Sciences, Japan. Flow cytometry reagents, including fixed malaria-infected rat blood (malaria biostandard) were from Rat MicroFlow^{PLUS} Kits contributed by Litron Laboratories (available from Litron Laboratories, Rochester, NY and BD Biosciences PharMingen, San Diego, CA).

Animals and treatment regimens. Animal studies were conducted in compliance with guidelines of the National Research Council (1996) "Guide for the Care and Use of Laboratory Animals" and were approved by the appropriate Institutional Animal Care and Use Committees. Two female Sprague-Dawley rats, 4- to 5-weeks old, were purchased from Taconic, Germantown, NY. Animals were housed singly and were assigned randomly to treatment groups. The animals were acclimated for approximately 2 weeks before the experiment was initiated. Food and water were available *ad libitum* throughout the acclimation and experimentation periods. One rat was treated via oral gavage with distilled water, and the other rat was treated by the same route with 10 mg CP/kg/day for 6 consecutive days.

Blood/bone marrow sample collection and storage. Each day, before vehicle or CP treatment, low-volume blood samples (approximately 100 µl) were collected from the tail vein using a 26.5-gauge needle and syringe after a brief warming period under a heat lamp. These samples were fixed for flow cytometric analysis of RET and MN-RET frequencies according to procedures described in the Rat MicroFlow^{PLUS} manual (v020213). Fixed samples were stored at − 85°C until analysis. Approximately 24 h after the last administration of vehicle or CP, blood samples were collected into tubes containing heparin solution (500 USP units heparin per milliliter of phosphate buffered saline) as follows: into a small tube containing 75 µl heparin solution, blood was collected until a final volume of approximately 750 µl was obtained; into a second tube containing 5 ml heparin solution, approximately 1 ml blood was collected. To tubes with the 750 µl blood suspension, an equal volume of heat-inactivated fetal bovine serum (FBS) was added. These FBS-diluted suspensions were used to prepare replicate AO-supravital (SV) slides (8 µl per slide) according to the method of Hayashi *et al.* (1990, 1992). These slides were frozen, shipped to collaborating SV-AO laboratories on dry ice, and stored frozen until analysis. FBS-diluted blood suspensions were also used to prepare slides for conventional acridine orange staining of methanol-fixed smears (MeOH-AO) staining (5 µl per slide). These blood smears were prepared by drawing the cell suspensions behind a second slide with smoothed edges (a "spreader slide"). These smears were allowed to air dry and were then fixed with absolute methanol for 10 min. The slides were stored in a slide box until they were shipped to collaborating MeOH-AO laboratories for MN scoring according to their standard operating procedures. Replicate bone marrow slides were prepared as smears, air dried, methanol fixed, and shipped similarly. These bone marrow cells were harvested from two femurs per rat, whereby both ends of each femur were cut and its contents flushed with 1 ml FBS. The cells were centrifuged at approximately at 1100 rpm for 5 min and then resuspended with approximately 600 µl FBS. As with the peripheral blood, 5 µl of cell suspension was applied to each slide. The 6 ml heparinized peripheral blood suspensions were fixed with ultracold methanol according to procedures described in the Rat MicroFlow^{PLUS} manual (v020213) in order to preserve cells for flow cytometric analysis. These cell suspensions were stored at − 85°C until analysis or shipment on dry ice to collaborating flow cytometry laboratories.

The samples obtained were divided into three identical pools, and replicate samples of each pool were provided to participating laboratories with three separate codes. Thus, laboratories received triplicate samples of each condition, but were not aware that they were from an identical pool. Thus, the analyses

conducted allow assessment of both intralaboratory variability of replicate analysis of identical samples and interlaboratory variability of the same analysis. Each laboratory also conducted analysis of each of these pools on three separate occasions, allowing assessment of variability of analysis over time.

Standard acridine orange slide scoring (MeOH-AO). Blood and bone marrow smears were scored using the MeOH-AO scoring technique at the Food and Drug Administration-National Center for Toxicological Research laboratory (L1) and three contract testing laboratories (L9, L10, and L11). Methanol fixation leads to a diffuse distribution of RNA, and erythrocytes are classified as normochromatic or as RETs based on the presence or absence of RNA-associated fluorescence. This technique is not well suited for visually classifying subpopulations of RETs. RET frequencies were determined by inspecting 500 or 1000 total erythrocytes per bone marrow or blood sample, respectively. MN-RET incidence was determined by inspecting 2000 RETs per sample. At L1, micronuclei were defined by the criteria of Schmid (1976) with the added requirements that they exhibit the characteristic yellow to yellow-green fluorescence characteristic of AO staining and that they exhibit the smooth boundary expected from a membrane-bound body. Laboratories L9, L10, and L11 were instructed to follow the standard operating procedures they use for regulatory submissions to support new drug or food additive development. Thus, the acquisition of data by these facilities allows for comparisons with three highly experienced contract laboratories under conditions associated with regulatory testing.

Supravital acridine orange slide scoring (SV-AO). Laboratories L5, L6, and L7 scored peripheral blood samples using the SV-AO scoring technique. This staining procedure aggregates RNA, leading to punctate staining patterns. These staining characteristics allow RET to be classified into four age cohorts: Type I (youngest) through Type IV (oldest) RETs as described by Hayashi *et al.* (1990, 1992). The frequency of MN-RETs was determined by analyzing 2000 Type I and Type II RETs (L5 and L7) or 2000 Type I RETs (L6). An index of cytotoxicity was obtained by inspecting at least 400 RETs and calculating the percentage of Type I and Type II RET among total RETs (L5 and L7) or the percentage of Type I RETs among Type I and Type II RETs (L6). AO-coated slides were purchased from TOYOBO (Osaka, Japan). Supravitally stained triplicate slides were frozen and sent to the Japanese reference laboratory (Nitto Denko) with dry ice. Each set of slides was also sent to two other laboratories for replicate scoring by fluorescence microscopy.

Flow cytometry–based scoring. Methanol-fixed blood samples were washed and labeled for flow cytometric analysis by L1, L2, and L3 according to procedures described in the Rat MicroFlow^{PLUS} Kit (v020213). Samples were analyzed with 488-nm capable instruments (FACSCalibur, FACSort, and FACScan, all from Becton Dickinson, San Jose, CA). Anti-CD71-FITC and propidium iodide fluorescence signals were detected in the FL1 and FL3 channels, respectively (stock filter sets). Calibration of the flow cytometers for the MN scoring application, across laboratories and between experiments within each laboratory, was accomplished by staining *Plasmodium berghei*–infected rat blood (malaria biostandards) in parallel with test samples on each day of analysis (Dertinger *et al.*, 2000; Tometsko *et al.*, 1993; Torous *et al.*, 2001). By adjusting voltages applied to the photomultiplier tube, it was possible to standardize the FL3 fluorescence channel into which erythrocytes with single (MN like) parasites fell. In this manner, analysis regions were consistent across laboratories and between experiments. Flow cytometry–based MN-RET measurements reported herein are based on an immature fraction of peripheral blood RETs (approximately the youngest 30–50% of propidium iodide–positive erythrocytes, based on CD71 expression level; Torous *et al.*, 2001, 2003). This is thought to be analogous to scoring the youngest (Types I and II) RETs using the SV-AO method, which may be beneficial in view of reports which have suggested that the influence of rat spleen filtration function can be minimized by scoring the younger RETs (Abramsson-Zetterberg *et al.*, 1999; Hayashi *et al.*, 1992; Hynes *et al.*, 2002; Torous *et al.*, 2000, 2003). Data were acquired with CellQuest software (v3.3, BD-Immunocytometry Systems, San Jose, CA), with the stop mode set so that 20,000 high CD71-expressing RETs were analyzed per blood sample. The number of mature (CD71 negative) erythrocytes was determined concurrently, providing an index of cytotoxicity (%RETs).

Calculations. All calculations were performed with Excel (Office X for Mac or Microsoft Office Excel 2002 for XP Windows Professional, Microsoft Corp., Seattle, WA). The incidences of MN-RETs are expressed as frequency percent. The percentage of RETs among total erythrocytes was measured by the flow cytometric and MeOH-AO laboratories and served as an index of bone marrow cytotoxicity. The three SV-AO laboratories used percentage of RETs in different stages of maturity as an index of toxicity; therefore, these indices are not directly comparable to those obtained by the flow cytometric and MeOH-AO microscopy laboratories. Percent coefficient of variance values (%CV, i.e., standard deviation (SD) as percent of the mean) were used to describe intralaboratory variability associated with multiple readings of replicate samples and also interlaboratory variation of vehicle control and CP-induced MN-RET measurements that were pooled according to scoring method.

RESULTS AND DISCUSSION

Confirmation of Steady State

RET and MN-RET measurements obtained from the daily low-volume blood specimens were analyzed to confirm that the

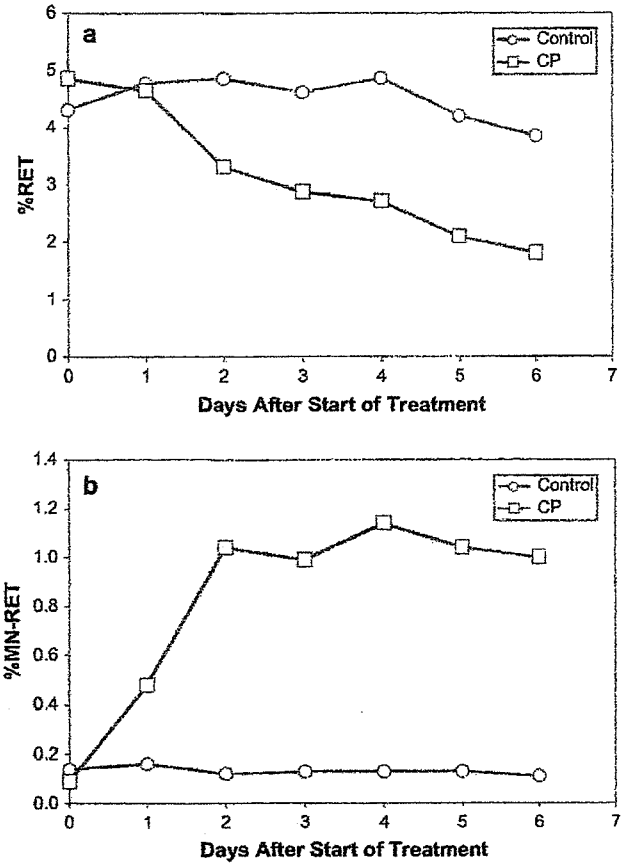

FIG. 1. The frequency of peripheral blood RETs (%RET, panel a) and peripheral blood micronucleated RETs (%MN-RET, panel b) as a function of time in the individual rats used to generate reference samples for analytical comparison. These data were acquired by flow cytometric analysis (laboratory L2) and demonstrate the attainment of a steady-state MN-RET frequency, facilitating subsequent comparisons between bone marrow and peripheral blood compartments.

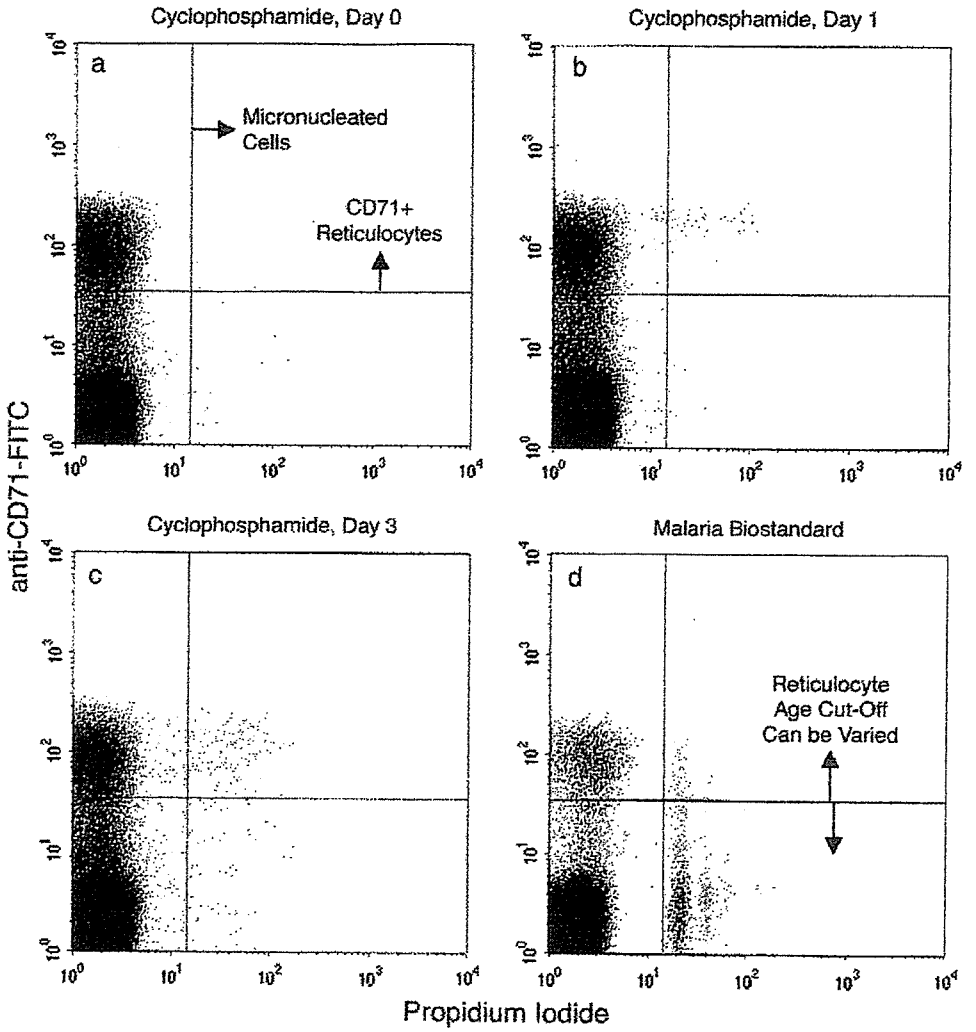

FIG. 2. Panels (a–c): Bivariate graphs illustrate the staining characteristics of rat blood specimens over the course of several days of CP treatment. Note the appearance of micronuclei at Day 1 in the very youngest (highest anti-CD71-FITC fluorescence) RETs (Panel b) and the more uniform distribution among RETs after a steady state has been reached on Day 3 of treatment (Panel c). Panel (d) illustrates the use of the malaria standard, with distinct fluorescence intensities corresponding to inclusion of one, two, or three parasites. This allows the instrument settings to be standardized to the DNA content of the parasite, which is controlled biologically to a quantity similar to that in an average MN.

MN-RET frequency of the vehicle-treated animal was stable over the duration of the experiment and that CP treatment caused the MN-RET frequency to increase to a steady-state level of approximately 10-fold the control frequency (Fig. 1). Since the frequency of MN-RETs was at steady state in both cases, the values in bone marrow and peripheral blood should be directly comparable—that is, expected to be equal in the absence of selective removal of MN-RETs from blood or methodological differences in measurement. Thus, the samples collected in this manner allow the direct comparisons between measurements in the bone marrow and blood compartments that follow. The use of large samples from a single treated and a single control rat allows differences in methodology and scoring laboratory to be assessed independently of sample variation.

The dose of CP (10 mg/kg/day) had a moderate effect on erythropoiesis, as indicated by the decline in RET frequency (terminal day specimen showed a greater than 50% decrease from pretreatment value; see Fig. 1, panel a). This level of bone marrow cytotoxicity is well within the range of target toxicity recommended by current regulatory guidances (i.e., $\leq$ 80%, see Organisation for Economic Cooperation and Development, 1997, Guideline 474; U.S. Food and Drug Administration, 2000.

To illustrate the nature and source of the flow cytometry–based data described above, bivariate fluorescence intensity plots are provided (Fig. 2). Note the appearance of micronuclei on Day 1 in the very youngest (highest anti-CD71-FITC fluorescence) RETs (Panel b) and the more uniform distribution

TABLE 2
Reticulocyte Data (cytotoxicity determinations)

Laboratory	Method	Compartment	Treatment	Cytotoxicity index[a]	Average %RET[b] ± SEM	%CV	%Change
L1	MeOH-AO	BM	Vehicle	%RET	81.0 ± 0.70	1.5	
			CP		67.8 ± 2.36	6.0	− 16
L9	MeOH-AO	BM	Vehicle	%RET	65.4 ± 1.03	2.7	
			CP		51.9 ± 1.83	6.1	− 21
L10	MeOH-AO	BM	Vehicle	%RET	58.2 ± 1.65	4.9	
			CP		60.0 ± 0.66	1.9	+ 3
L11	MeOH-AO	BM	Vehicle	%RET	63.1 ± 1.67	4.6	
			CP		57.1 ± 1.14	3.5	− 10
Pooled[b] L1, 9, 10, 11			***Vehicle***		***66.9 ± 2.63***	***13.6***	
			CP		***59.2 ± 1.87***	***10.9***	***− 12***
L1	MeOH-AO	PB	Vehicle	%RET	7.7 ± 0.19	4.2	
			CP		5.7 ± 0.27	8.2	− 26
L9	MeOH-AO	PB	Vehicle	%RET	6.2 ± 0.27	7.4	
			CP		5.6 ± 0.90	27.8	− 9
L11	MeOH-AO	PB	Vehicle	%RET	6.6 ± 0.52	13.5	
			CP		4.9 ± 0.33	11.7	− 26
Pooled L1, 9, 11			***Vehicle***		***6.9 ± 0.29***	***12.5***	
			CP		***5.4 ± 0.32***	***17.6***	***− 21.7***
L5	SV-AO	PB	Vehicle	%Type I + II/I–IV	55.2 ± 1.95	6.1	
			CP		42.2 ± 0.12	0.5	− 24
L6	SV-AO	PB	Vehicle	%Type I/I + II	42.4 ± 2.8	11.5	
			CP		29.1 ± 2.1	12.4	− 31
L7	SV-AO	PB	Vehicle	%Type I + II/I–IV	52.3 ± 2.1	6.8	
			CP		34.8 ± 3.1	15.6	− 34
Pooled[c] L5, 7			***Vehicle***		***53.7 ± 1.4***	***6.5***	
			CP		***38.5 ± 2.2***	***13.8***	***− 28***
L1	FCM	PB	Vehicle	$\%RET^{High\ CD71+}$	3.40 ± 0.02	1.18	
			CP		1.53 ± 0.01	0.75	− 55
L2	FCM	PB	Vehicle	$\%RET^{High\ CD71+}$	3.32 ± 0.02	1.26	
			CP		1.44 ± 0.01	1.44	− 57
L3	FCM	PB	Vehicle	$\%RET^{High\ CD71+}$	3.32 ± 0.05	2.42	
			CP		1.40 ± 0.08	9.88	− 58
Pooled L1, 2, 3			***Vehicle***		***3.34 ± 0.02***	***1.93***	
			CP		***1.46 ± 0.03***	***6.33***	***− 56***

Note. Abbreviations: RET = reticulocyte; MeOH-AO = acridine orange staining of methanol-fixed smears; SV-AO = supravital staining using acridine orange–coated slides; FCM = flow cytometry; BM = bone marrow; PB = peripheral blood; CP = cyclophosphamide; SEM = standard error of the mean.

[a]Each laboratory evaluated cytotoxicity based on immature erythrocyte parameters. This was accomplished in several different manners: %RET = percentage of RETs relative to total erythrocytes; %Type I + II/I–IV = percentage of Type I and Type II RETs relative to total RETs; %Type I/I + II = percentage of Type I RETs relative to Type I and Type II RETs; and $\%RET^{High\ CD71}$ = percentage of RETs that express high levels of CD71 relative to total erythrocytes.

[b]Values are the mean of three separately coded, but identical, samples. By "Pooled" it is meant that like-method data from two, three, or four laboratories were combined for these calculations.

[c]Only data from the two SV-AO laboratories that measured toxicity similarly (%Type I + II/I–IV) were combined for these calculations.

among RETs after a steady state has been reached on Day 3 of treatment (Panel c). Panel (d) illustrates the use of the malaria biostandard, with distinct fluorescence intensities corresponding to inclusion of one, two, or three parasites. This allows the instrument settings to be standardized to the DNA content of the parasite, which is controlled biologically to a quantity similar to that in an average MN. For research purposes, the regions may be adjusted to allow measurements in different age populations of RETs and/or micronuclei with different DNA contents. For analytical purposes, the standard can be used to achieve comparable instrument performance across time within a laboratory or across different instruments in different laboratories.

Intra- and Interlaboratory Variability

Replicate bone marrow and/or peripheral blood specimens obtained after 6 consecutive days of treatment were provided to each collaborating laboratory. As noted above, the frequencies of MN-RETs were at steady state and therefore not changing as a function of time. Each laboratory received three separately coded samples from each of the high and low MN-RET frequency pools but were not aware that the three separately coded samples were identical. Tabular values are the means of the values of the three separately coded samples.

TABLE 3
Intra- and Interlaboratory Micronucleated Reticulocyte Data

Laboratory	Method	Compartment	Treatment	%MN-RET Average[a] ± SEM	%CV	Fold difference
L1	MeOH-AO	BM	Vehicle	0.15 ± 0.03	33.3	
			CP	3.35 ± 0.10	5.4	22.3
L9	MeOH-AO	BM	Vehicle	0.05 ± 0.05	173.2	
			CP	1.63 ± 0.27	28.4	32.6
L10	MeOH-AO	BM	Vehicle	0.03 ± 0.02	86.6	
			CP	2.33 ± 0.23	17.3	77.7
L11	MeOH-AO	BM	Vehicle	0.18 ± 0.03	31.5	
			CP	2.44 ± 0.20	13.9	13.6
Pooled[a] L1, 9, 10, 11			***Vehicle***	***0.10 ± 0.02***	***80.5***	
			CP	***2.44 ± 0.21***	***29.1***	***24.4***
L1	MeOH-AO	PB	Vehicle	0.05 ± 0.03	100.0	
			CP	1.77 ± 0.17	16.6	35.4
L9	MeOH-AO	PB	Vehicle	0.05 ± 0.00	0.0	
			CP	0.50 ± 0.03	10.0	10.0
L11	MeOH-AO	PB	Vehicle	0.18 ± 0.04	41.7	
			CP	1.42 ± 0.10	12.3	7.9
Pooled L1, 9, 11			***Vehicle***	***0.09 ± 0.03***	***85.6***	
			CP	***1.23 ± 0.20***	***48.2***	***13.7***
L5	SV-AO	PB	Vehicle	0.13 ± 0.03	43.3	
			CP	1.83 ± 0.15	13.7	14.1
L6	SV-AO	PB	Vehicle	0.12 ± 0.07	99.0	
			CP	1.77 ± 0.32	31.2	14.8
L7	SV-AO	PB	Vehicle	0.22 ± 0.14	113.8	
			CP	1.47 ± 0.27	31.7	6.7
Pooled L5, 6, 7			***Vehicle***	***0.16 ± 0.05***	***94.3***	
			CP	***1.69 ± 0.14***	***24.7***	***10.6***
L1	FCM	PB	Vehicle	0.12 ± 0.02	24.8	
			CP	0.99 ± 0.04	6.5	8.3
L2	FCM	PB	Vehicle	0.11 ± 0.02	31.5	
			CP	1.04 ± 0.04	6.7	9.5
L3	FCM	PB	Vehicle	0.11 ± 0.02	32.9	
			CP	1.11 ± 0.04	6.8	10.1
Pooled L1, 2, 3			***Vehicle***	***0.11 ± 0.01***	***26.5***	
			CP	***1.05 ± 0.03***	***7.6***	***9.5***

Note. Abbreviations: MN-RET = micronucleated reticulocyte; MeOH-AO = acridine orange staining of methanol-fixed smears; SV-AO = supravital staining using acridine orange–coated slides; FCM = flow cytometry; BM = bone marrow; PB = peripheral blood; CP = cyclophosphamide; SEM = standard error of the mean; %CV = percent coefficient of variance.

[a]Values are the mean of three separately coded, but identical, samples. By "Pooled" it is meant that like-method data from three or four laboratories were combined for these calculations.

Most laboratories detected a reduction in %RET for the CP-treated rat (see Table 2). However, this was somewhat variable across microscopy-based laboratories, especially when the MeOH-AO technique was used to evaluate bone marrow specimens. In two of the three laboratories that scored both bone marrow and peripheral blood, peripheral blood measurements demonstrated greater CP-associated reduction of %RETs than in bone marrow. Intra- and interlaboratory %CV values for the replicate RET analyses are presented in Table 2. Flow cytometric measurements were more consistent within and across laboratories than microscopic scoring. For instance, vehicle control specimens' %CV for pooled laboratory MeOH-AO/bone marrow data was 13.6%, while the corresponding blood-based analyses for flow cytometric, SV-AO, and MeOH-AO techniques were 1.93, 6.5, and 12.5%, respectively.

The interlaboratory %CV values for MN-RET determinations and the intralaboratory %CV values for the triplicate blinded analyses conducted within each laboratory are provided in Table 3. The flow cytometric analyses demonstrate superior intra- and interlaboratory consistency relative to both microscopy-based methods. %CV values for MN-RET measurements performed on vehicle control blood specimens pooled across like-method laboratories were 26.5, 94.3, and 85.6% for the flow cytometric, SV-AO, and MeOH-AO methods, respectively, and 80.5% for MeOH-AO scored bone marrow. Analogous %CV values for CP blood samples were 7.6, 24.7,

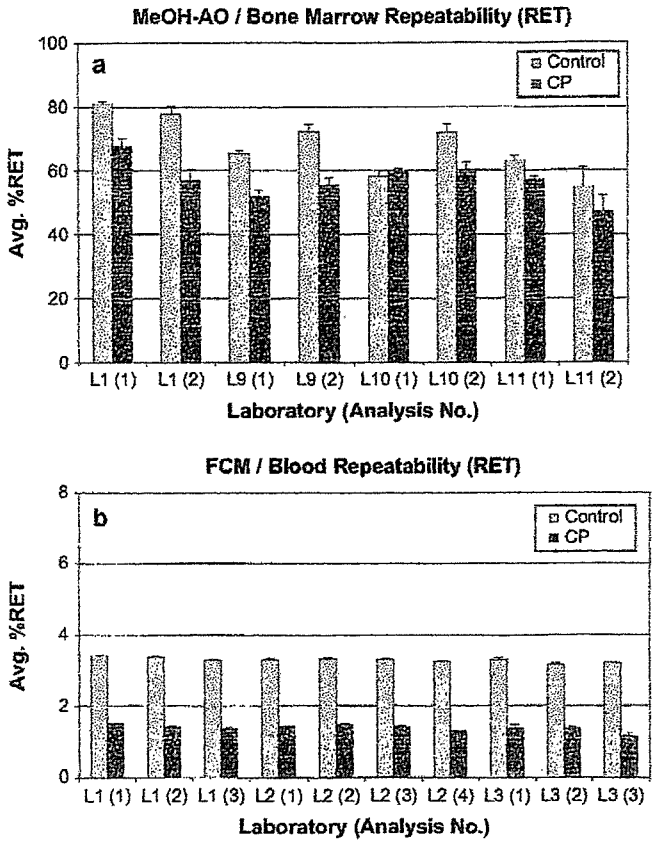

FIG. 3. Values are the mean of three identical, but separately coded, samples. Panel (a): The average frequency of bone marrow RETs (%RET) as measured by the standard MeOH-AO microscopy technique are graphed (with standard error of mean [SEM] bars). These data were collected on two separate occasions at each laboratory. Panel (b): The average frequency of peripheral blood RET as measured by the flow cytometric (FCM) technique are graphed (with SEM bars). These data were collected on three or four separate occasions.

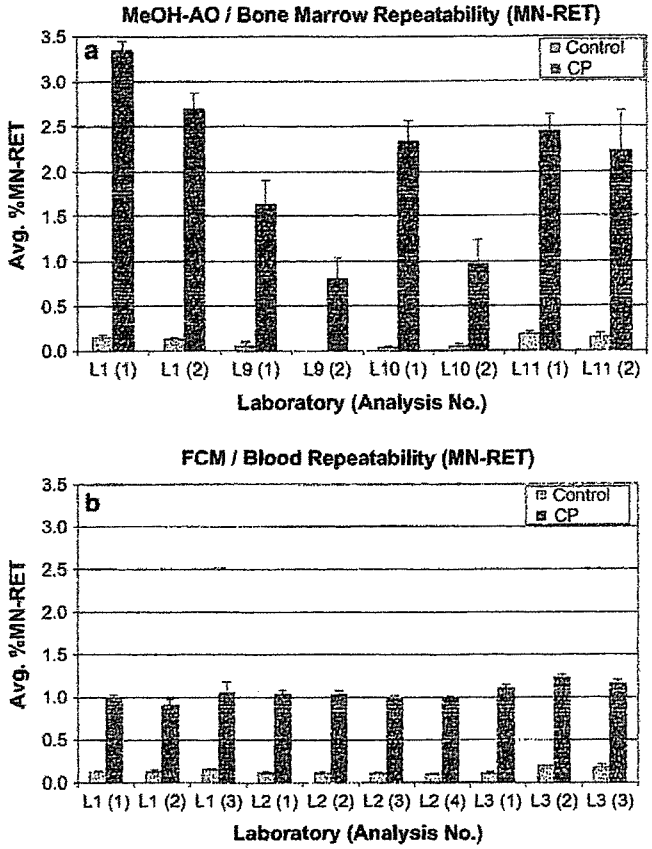

FIG. 4. Values are the mean of three identical, but separately coded, samples. Panel (a): The average frequency of bone marrow micronucleated RETs (%MN-RET) as measured by the standard MeOH-AO microscopy technique are graphed (with standard error of mean [SEM] bars). These data were collected on two separate occasions at each laboratory. Panel (b): The average frequency of peripheral blood MN-RET as measured by the flow cytometric (FCM) technique are graphed (with SEM bars). These data were collected on three or four separate occasions.

and 48.2%, respectively, and 29.1% for MeOH-AO scored bone marrow.

Fold difference values based on each laboratory's average MN-RET frequencies, as well as for like-method pooled data, are also presented (Table 3). It was somewhat surprising that the fold difference in MN-RETs between vehicle and CP-associated blood specimens, as well as absolute MN-RET frequencies, were no higher with the flow cytometric or SV-AO techniques than with the conventional MeOH-AO method as it has been reported that restriction of MN analysis to an immature RET cohort based on RNA content or CD71 expression levels could reduce, if not eliminate, the influence of the spleen's erythrophagocytotic activity (Abramsson-Zetterberg *et al.*, 1999; Hayashi *et al.*, 1992). Splenic activity and its effects on assay sensitivity for blood-based analyses have been investigated thoroughly, and these data are discussed in a companion paper that appears in this issue (MacGregor *et al.*).

Intralaboratory Variability Across Time

In addition to the inter- and intralaboratory analyses, an evaluation of scoring reproducibility over time was studied. This was accomplished by having flow cytometry laboratories analyze coded peripheral blood specimens on three or four different occasions, while triplicate vehicle and CP bone marrow slides were submitted to L9, L10, and L11 laboratories for analysis on two separate occasions. Reagents were prepared separately for each day of analysis. The resulting repeat-analysis RET data are presented in Figure 3 and demonstrate higher reproducibility for the multiple flow cytometric analyses compared to MeOH-AO.

As with RET enumeration, repeat-analysis MN-RET microscopy data were also quite variable. For instance, laboratories using the MeOH-AO method reported average CP-induced values that differed from their original mean reading by 19.4,

50.9, 58.4, and 8.6% (L1, L9, L10, and L11, respectively; see Fig. 4). Repeat-analysis MN-RET data generated by the flow cytometric technique were considerably more reproducible as average values were all within 11% of the originally reported mean frequencies. It should also be noted that the fourth flow cytometric analyses by L2 was performed more than 2 years after blood fixation, demonstrating this procedure's compatibility with long-term storage of fixed blood specimens.

CONCLUSIONS

Distribution of replicate bone marrow and blood specimens obtained from single rats that were first shown to exhibit steady-state spontaneous or genotoxicant-induced MN-RET frequencies were used to assess inter- and intralaboratory scoring variability using two widely used microscopic and one flow cytometric procedure. These results demonstrate that the quantification of MN-RETs benefits from an objective flow cytometry–based method of data acquisition. The flow cytometric method provides better reproducibility, and the high throughput capability allows interrogation of tens of thousands of RETs per specimen. Enhanced scoring precision is important as it is necessary to offset the spleen-dependent loss of dynamic range observed in peripheral blood relative to bone marrow—a phenomenon that was observed in this as well as other reports (MacGregor *et al.*, this issue; Wakata *et al.*, 1998). A recent report by Torous *et al.* (2006) delincates the consequential improvements to assay power when the number of cells scored per specimen is increased and supports this view.

Beyond overcoming lower genotoxicant-induced MN-RET frequencies in blood relative to bone marrow, further incentive for automating rat peripheral blood MN-RET measurements comes from a recent recommendation of the *In Vivo* MN Assay Expert Group of the International Working Group on Genetic Toxicology Testing (IWGT; Hayashi *et al.*, in press). Specifically, IWGT has recommended that a sufficient number of RETs should be scored to ensure that the MN-RET counting error is kept below the level of interanimal variability. This allows the sensitivity of the experiment to be limited by the variability of spontaneous MN-RET frequency among animals, rather than being limited by the statistical variation of count. Based on the flow cytometric scoring of 20,000 peripheral blood RETs from each of the 15 control animals from the three experiments reported in the MacGregor *et al.* companion paper in this issue (laboratory L2, the reference laboratory), we find that the mean incidence of MN-RET ± 1 SD is 0.11% ± 0.045. This is a 41% CV. Poisson distribution theory allows us to calculate that 6 MN-RETs per animal must be scored to limit counting error to this level of variation (SD of the Poisson count = $\sqrt{\text{absolute count}}$). At a spontaneous MN-RET frequency of approximately 0.1%, this means that an average of 6000 RETs per individual need to be scored for micronuclei in order to achieve a CV that is at or below the interanimal variance. This is a significantly higher number of RETs per animal than required to be scored under the current OECD MN assay guideline (which recommends scoring 2000 RETs per animal) and is difficult to achieve by manual microscopic scoring.

In conclusion, the data presented herein and in the companion paper that follows support the growing consensus that rat peripheral blood can be used to perform *in vivo* MN tests more effectively than the standard bone marrow–based assay. The ability of the described automated scoring procedure to greatly enhance the precision of MN-RET measurements overcomes the somewhat attenuated genotoxicant-induced frequencies observed in peripheral blood relative to bone marrow. This conclusion is supported by experiments described in the accompanying paper whereby intact and splenectomized rats were treated with diverse genotoxicants (MacGregor *et al.*, this issue).

ACKNOWLEDGMENTS

This work was supported by an intercenter research award from the Food and Drug Administration Office of Science and Health Coordination to J.T.M. The contents are the sole responsibility of the authors and do not necessarily represent the official views of the U.S. Food and Drug Administration, the National Institute of Health Sciences, Japan, or Health Canada. We would like to thank Nikki Hall for her expert assistance with bleeding and dosing procedures. Thanks also to Puntipa Kwanyuen and Dr Neal Cariello, two researchers who were early adopters of the flow cytometric technique described herein. Their experiences with an early version of the method led to the development of malaria-infected erythrocytes as daily calibration standards. Conflict of interest disclosure: Litron Laboratories holds patents pertaining to flow cytometric enumeration of micronucleated erythrocyte populations and also sells kits that facilitate these analyses. The authors express their appreciation for the cooperation and contributions of the staff of the 3 contract laboratories that participated in these studies: Drs Robert Young and Rama Gudi of BioReliance, Rockville, MD; Dr Gregory Erexson of Covance, Inc., Vienna, VA; and Dr John Mirsalis and Edward Riccio of SRI International, Menlo Park, CA.

REFERENCES

Abramsson-Zetterberg, L., Grawe, J., and Zetterberg, G. (1999). The micronucleus test in rat erythrocytes from bone marrow, spleen and peripheral blood: The response to low doses of ionizing radiation, cyclophosphamide and vincristine determined by flow cytometry. *Mutat. Res.* **423,** 113–124.

Asanami, S., Shimono, K., Sawamoto, O., Kurisu, K., and Uejima, M. (1995). The suitability of rat peripheral blood in subchronic studies for the micronucleus assay. *Mutat. Res.* **347,** 73–78.

Dertinger, S. D., Camphausen, K., MacGregor, J. T., Bishop, M. E., Torous, D. K., Avlasevich, S., Cairns, S., Tometsko, C. R., Menard, C., Muanza, T., *et al.* (2004). Three-color labeling method for flow cytometric measurement of cytogenetic damage in rodent and human blood. *Environ. Mol. Mutagen.* **44,** 427–435.

Dertinger, S. D., Torous, D. K., Hall, N. E., Tometsko, C. R., and Gasiewicz, T. A. (2000). Malaria-infected erythrocytes serve as biological standards to ensure reliable and consistent scoring of micronucleated erythrocytes by flow cytometry. *Mutat. Res.* **464,** 195–200.

Hamada, S., Sutou, S., Morita, T., Wakata, A., Asanami, S., Hosoya, S., Ozawa, S., Kondo, K., Nakajima, M., Shimada, H., *et al.* (2001). Evaluation of the rodent micronucleus assay by a 28-day treatment protocol: Summary of the 13th collaborative study by the collaborative study group for the micronucleus test (CSGMT)/Environmental Mutagen Society of Japan (JEMS)—Mammalian Mutagenicity Study Group (MMS). *Environ. Mol. Mutagen.* **37,** 93–110.

Hayashi, M., Kodama, Y., Awogi, T., Suzuki, T., Asita, A. O., and Sufuni, T. (1992). The micronucleus assay using peripheral blood reticulocytes from mitomycin C- and cyclophosphamide-treated rats. *Mutat. Res.* **278,** 209–213.

Hayashi, M., MacGregor, J. T., Gatehouse, D. G., Adler, I.-D., Blakey, D. H., Dertinger, S. D., Krishna, G., Morita, T., Russo, A., and Sutou, S. (2000). *In vivo* rodent erythrocyte micronucleus assay: Aspects of protocol design including repeated treatments, integration with toxicity testing, and automated scoring. A report from the International Workshop on Genotoxicity Test Procedures (IWGTP). *Environ. Mol. Mutagen.* **35,** 234–252.

Hayashi, M., MacGregor, J. T., Gatehouse, D. G., Blakey, D. H., Dertinger, S. D., Abramsson-Zetterberg, L., Krishna, G., Morita, T., Russo, A., Asano, N., *et al. In vivo* erythrocyte micronucleus assay: III. Validation and regulatory acceptance of automated scoring and the use of rat peripheral blood reticulocytes, with discussion of non-hematopoietic target cells and a single dose-level limit test. *Environ. Mol. Mutagen.* (in press).

Hayashi, M., Morita, T., Kodama, Y., Sofuni, T., and Ishidate, M., Jr. (1990). The micronucleus assay with mouse peripheral blood reticulocytes using acridine orange-coated slides. *Mutat. Res.* **245,** 245–249.

Hynes, G. M., Torous, D. K., Tometsko, C. R., Burlingson, B., and Gatehouse, D. G. (2002). The single laser flow cytometric micronucleus test: A time course study using colchicines and urethane in rat and mouse peripheral blood and acetaldehyde in rat peripheral blood. *Mutagenesis* **17,** 15–23.

MacGregor, J. T., Tucker, J. D., Eastmond, D. A., and Wyrobek, A. J. (1995). Integration of cytogenetic assays with toxicology studies. *Environ. Mol. Mutagen.* **25,** 328–337.

MacGregor, J. T., Wehr, C. M., Hiatt, R. A., Peters, B., Tucker, J. D., Langlois, R. G., Jacob, R. A., Jenson, R. H., Yager, J. W., Shigenaga, M. K., *et al.* (1997). "Spontaneous" genetic damage in man: Evaluation of interindividual variability, relationship among markers of damage, and influence of nutritional status. *Mutat. Res.* **377,** 125–135.

Organisation for Economic Cooperation and Development (OECD) (1997). OECD Guideline 474. Guideline for the testing of chemicals. Mammalian erythrocyte micronucleus test.

Romagna, F., and Staniforth, C. D. (1989). The automated bone marrow micronucleus test. *Mutat. Res.* **213,** 91–104.

Schmid, W. (1976). The micronucleus test for cytogenetic analysis. In *Chemical Mutagens: Principles and Methods for their Detection,* A. Hollaender, (Ed.) Vol. 4, pp. 31–53. Plenum Press, New York.

Tometsko. A. M., Torous, D. K., and Dertinger, S. D. (1993). Analysis of micronucleated cells by flow cytometry. 1. Achieving high resolution with a malaria model. *Mutat. Res.* **292,** 129–135.

Torous, D., Asano, N., Tometsko, C., Sugunan, S., Dertinger, S., Morita, T., and Hayashi, M. (2006). Performance of flow cytometric analysis for the micronucleus assay—A reconstruction model using serial dilutions of malaria infected cells with normal mouse peripheral blood. *Mutagenesis* **21,** 11–13.

Torous, D. K., Dertinger, S., Hall, N., and Tometsko, C. (2000). Enumeration of micronucleated reticulocytes in rat peripheral blood: A flow cytometric study. *Mutat. Res.* **465,** 91–99.

Torous, D. K., Hall, N. E., Dertinger, S. D., Diehl, M., Illi-Love, A. H., Cederbrant, K., Sandelin, K., Bolcsfoldi, G., Ferguson, L. R., Pearson, A., *et al.* (2001). Flow cytometric enumeration of micronucleated reticulocytes: High transferability among 14 laboratories. *Environ. Mol. Mutagen.* **38,** 59–68.

Torous, D. K., Hall, N. E., Murante, F. G., Gleason, S. E., Tometsko, C. R., and Dertinger, S. D. (2003). Comparative scoring of micronucleated reticulocytes in rat peripheral blood by flow cytometry and microscopy. *Toxicol. Sci.* **74,** 309–314.

U.S. Food and Drug Administration (2000) Office of Food Additive Safety, Redbook (2000). Toxicological Principals for the Safety Assessment of Food Ingredients. Available at: http://www.cfsan.fda.gov/~redbook/red-toca.html. Updated on November 2003. U.S. Food and Drug Administration, Washington, D.C.

Wakata, A., Miyamae, Y., Sato, S., Suzuki, T., Morita, T., Asano, N., Awogi, T., Kondo, K., and Hayashi, M. (1998). Evaluation of the rat micronucleus test with bone marrow and peripheral blood: Summary of the 9th collaborative study by CSGMT/JEMS.MMS. *Environ. Mol. Mutagen.* **32,** 84–100.

Glycobiology Advance Access published January 12, 2007

Comparison of the Methods for Profiling Glycoprotein Glycans: HUPO HGPI (Human Proteome Organisation Human Disease Glycomics/Proteome Initiative) Multi-institutional Study

Yoshinao Wada[1], Parastoo Azadi[2], Catherine E. Costello[3], Anne Dell[4], Raymond A. Dwek[5], Hildegard Geyer[6], Rudolf Geyer[6], Kazuaki Kakehi[7], Niclas G. Karlsson[8,9], Koichi Kato[10], Nana Kawasaki[11], Kay-Hooi Khoo[12], Soohyun Kim[13], Akihiro Kondo[14], Erika Lattova[15], Yehia Mechref[16], Eiji Miyoshi[17], Kazuyuki Nakamura[18], Hisashi Narimatsu[19], Milos V. Novotny[20], Nicolle H. Packer[8], Hélène Perreault[15], Jasna Peter-Katalinić[20], Gottfried Pohlentz[20], Vernon N. Reinhold[21], Pauline M. Rudd[5,22], Akemi Suzuki[23] & Naoyuki Taniguchi[17,24]

[1]Osaka Medical Center and Research Institute for Maternal and Child Health, 840 Murodo-cho, Izumi, Osaka 594-1101, Japan. [2]Complex Carbohydrate Research Center, University of Georgia, 315 Riverbend Road, Athens, GA 30602-4712 USA. [3]Mass Spectrometry Resource, Department of Biochemistry, Boston University School of Medicine, 670 Albany Street, Boston, MA 02118-2646, USA. [4]Division of Molecular Biosciences, Imperial College, London SW7 2AZ, UK. [5]Oxford Glycobiology Institute, Department of Biochemistry, University of Oxford, South Parks Road, Oxford OX1 3QU, UK. [6]Institute of Biochemistry, University of Giessen, Friedrichstrasse 24, D-35392 Giessen, Germany. [7]Faculty of Pharmaceutical Sciences, Kinki University, Kowakae 3-4-1, Higashiosaka-shi, Osaka 577-8502, Japan. [8]Proteome Systems Limited, Unit 1, 35-41 Waterloo Road, North Ryde, Sydney, NSW 2113, Australia. [9]Chemistry Department, National University Ireland-Galway, Galway, Ireland [10]Graduate School of Pharmaceutical Sciences, Nagoya City University, 3-1 Tanabe-dori, Mizuho-ku, Nagoya 467-8603, Japan. [11]Division of Biological Chemistry and Biologicals, National Institute of Health Sciences, 1-18-1 Kami-yoga, Setagaya-Ku, Tokyo 158-8501, Japan. [12]Institute of Biological Chemistry, Academia Sinica, Taipei 115, Taiwan. [13]Glycomics Team, Korea Basic Science Institute, 52 Eoun-dong, Daejeon 305-333, Korea. [14]Department of Glycotherapeutics, Osaka University Graduate School of Medicine, Osaka 565-0871, Japan. [15]Department of Chemistry, University of Manitoba, Winnipeg, Manitoba R3T 2N2, Canada. [16]Department of Chemistry, Indiana University, Bloomington, IN 47405, USA. [17]Department of Biochemistry, Osaka University Graduate School of Medicine, Osaka 565-0871, Japan. [18]Department of Biochemistry and Biomolecular Recognition, Yamaguchi University School of Medicine, Minami-Kogushi, Ube, Yamaguchi 755-8505, Japan. Continued over page/

© The Author 2007. Published by Oxford University Press. All rights reserved.
For permissions, please e-mail: journals.permissions@oxfordjournals.org

[19]Research Center for Glycoscience (RCG), National Institute of Advanced Industrial Science and Technology (AIST), Open Space Laboratory Central-2, 1-1-1 Umezono, Tsukuba, Ibaraki 305-8568, Japan. [20]Institute for Medical Physics and Biophysics University of Münster, Robert-Koch-Str. 31 D-48149, Münster, Germany. [21]Department of Chemistry, University of New Hampshire, Durham, New Hampshire 03824, USA. [22]NIBRT, Conway Institute, University College Dublin, Belfield, Dublin 4, Ireland. [23]RIKEN Frontier Research System, 2-1 Hirosawa, Wako-shi, Saitama, 351-0198, Japan. [24]Department of Disease Glycomics, Research Institute for Microbial Diseases, Osaka University, Osaka 565-0871, Japan.

Mass spectrometry (MS) of glycoproteins is an emerging field in proteomics, poised to meet the technical demand for elucidation of the structural complexity and functions of the oligosaccharide components of molecules. Considering the divergence of the mass spectrometric methods employed for oligosaccharide analysis in recent publications, it is necessary to establish technical standards and demonstrate capabilities. In the present study of the HUPO HGPI (Human Proteome Organisation Human Disease Glycomics/Proteome Initiative), the same samples of transferrin and immunoglobulin-G were analyzed for *N*-linked oligosaccharides and their relative abundances in 20 laboratories, and the chromatographic and mass spectrometric analysis results were evaluated. In general, matrix-assisted laser desorption/ionization (MALDI) time-of-flight MS of permethylated oligosaccharide mixtures carried out in six laboratories yielded good quantitation, and the results can be correlated to those of chromatography of reductive amination derivatives. For underivatized oligosaccharide alditols, graphitized carbon-liquid chromatography (LC)/electrospray ionization (ESI) MS detecting deprotonated molecules in the negative ion mode provided acceptable quantitation. The variance of the results among these three methods was small. Detailed analyses of tryptic glycopeptides employing either nanoLC/ESI MS/MS or MALDI MS demonstrated the excellent capability to determine site-specific or subclass-specific glycan profiles in these samples. Taking into account the variety of MS technologies and options for distinct protocols used in this study, the results of this multi-institutional study indicate that MS-based analysis appears as the efficient method for identification and quantitation of oligosaccharides in glycomic studies and endorse the power of MS for glycopeptide characterization with high sensitivity in proteomic programs.

Glycosylation is a common post-translational modification providing a highly diverse structure variation to more than half of all secretory and cellular proteins (Apweiler, 1999). Several lines of evidence have indicated that attachment of a specific monosaccharide to core glycans or branches changes glycoprotein function, and the resulting transformation of cellular phenotypes is suggested to be involved in various biological or pathological processes such as cancer, infection, and reproduction (Taniguchi *et al.*, 2001; Hakomori, 2002; Helenius and Aebi, 2004). From a pharmacological point of view, glycosylation profoundly affects biological activity, function, clearance from the circulation, and crucially, the antigenicity of recombinant proteins (Brooks, 2004; Jefferis, 2005). Increasing knowledge of the biological significance of glycosylation has resulted from the development of analytical methods, among which mass spectrometry (MS) is an essential tool as it allows rapid and high sensitivity profiling and detailed characterization of heterogeneous glycan structures. In fact, in recent years, mass spectrometric analysis by soft ionization techniques, electrospray ionization (ESI)

or matrix-assisted laser desorption/ionization (MALDI), has been employed in most studies of oligosaccharide structure (Harvey, 1999; Dell and Morris, 2001; Mechref and Novotny, 2002; Zaia, 2004).

The capability of MS and data interpretation is based on various instrumental factors. For example, the physicochemical properties such as charge and internal energy of generated ions are largely dependent on the ionization methods employed. Different types of mass analyzers have specific time frames for detection and this affects the fragmentation patterns observed in the mass spectrum. Moreover, there are still other factors to consider with oligosaccharides such as derivatization, ion polarity and the nature of ion species derived from protonation and deprotonation, alkali-metal cations and different anion adduction. Although all of these factors affect, to varying extents, the relative intensities of the molecular ions for different oligosaccharide structures, it is also true that good quantitation can be expected with appropriately designed measurements, as already reported (Viseux *et al.*, 2001). While detailed reviews of current mass spectrometric techniques and analysis workflow are available, the emerging need for rapid and sensitive analysis of glycoprotein glycans makes it desirable to compare the performance of standard method(s). To this end, the HUPO HGPI (Human Proteome Organisation Human Disease Glycomics/Proteome Initiative) has formed a consortium with expertise in glycobiology, and has distributed *N*-glycosylated protein samples, transferrin and immunoglobulin-G (IgG) from healthy individuals to participating members for analysis. The released oligosaccharides were analyzed by MS or conventional chromatography, and in some cases, glycopeptides obtained by enzymatic proteolysis were also analyzed by MS. This report describes these analyses of glycoprotein glycans, focusing mainly on relative quantitative profiling of structural heterogeneity.

RESULTS

The laboratories enrolled in this study analyzed released oligosaccharides or glycopeptides, or both. The methods are summarized in Table 1. [The laboratory numbers designated in Table 1 and the succeeding figures are not the same as those given to the authors in the title.]

Human transferrin contains two *N*-linked complex type oligosaccharides at Asn-432 and Asn-630 (Spik *et al.*, 1975). Human IgG has a conserved *N*-linked glycosylation site, Asn-297, in the heavy chain of the Fc region, with variable glycosylation in the Fab depending on the presence or absence of the glycosylation motif in the variable region. The oligosaccharides attached within the Fc region are of a complex type (Takahashi *et al.*, 1987), showing higher heterogeneity than transferrin, and were the subject of this study.

For transferrin, the evaluation was primarily focused on the *N*-acetylneuraminic (sialic) acid levels. Sialic acids are major residues giving negative charge to the molecule and play a key role in various biological processes such as infection and cellular communication. The rather labile glycosidic linkage of sialic acid to the oligosaccharide chain can be cleaved during sample preparation or analysis thus making quantitation difficult. For IgG,

galactosylation levels were evaluated because of the possible alterations implicated in pathological conditions (Axford, 1999). In these respects, detection of minor glycans, specifically, the fucosylation and triantennary branching of the transferrin glycans and the bisecting *N*-acetylglucosamination of IgG glycans, was evaluated.

In addition, in the glycopeptide analysis, different oligosaccharide profiles at two glycosylation sites of transferrin and those of different IgG subclass molecules were identified.

Chromatographic analysis

Chromatography of reductively aminated oligosaccharides is generally accepted as a standard method of quantitation, in which the fluorescence correlates with the amounts of individual components. In the present study, five laboratories carried out this type of analysis utilizing 2-aminopyridine, 2-aminobenzamide or 2-aminobenzoate, as the labeling agent (Table 1), and the results were compared with those obtained by MS.

The chromatographic measurements of the oligosaccharides from sample A transferrin are summarized in Figure 1a (labs 1-4), in which the relative abundances of differently sialylated biantennary chains and trisialo-triantennary and fucosylated disialo-biantennary chains in the total oligosaccharides are presented. One laboratory (lab-1) discriminated the monosialo-binatennary isomers bearing a sialic acid at either antenna, and the values were summed for data presentation. In labs 1-4, the levels of monosialo- and disialo-biantennary, fucosylated disialo-biantennary and trisialo-triantennary chains were 7.6 ± 7.0, 70.8 ± 12.3, 5.1 ± 2.9 and 9.7 ± 7.5 (mean ± SD, %), respectively, apparently showing a considerable variance among reports. No laboratories detected significant amounts of the asialo-biantennary chain.

A majority of IgG oligosaccharides are of the fucosylated biantennary type, and are partially galactosylated. The contents of each differently galactosylated species among total fucosylated biantennary oligosaccharides from sample B IgG were calculated and are shown in Figure 2a (labs 1-5). Two laboratories (labs-1 and 5) discriminated the isomers with a galactose at either antenna, and the values were combined and represented by the monogalactosyl species. The most abundant structure was the monogalactosyl form, in three reports, while it was either agalactosyl or digalactosyl species in other laboratories. The number of galactose residues in a fucosylated biantennary oligosaccharide from this sample ranged from 0.82 (lab-3) to 1.59 (lab-4), and had a mean of 1.16 ± 0.28 for the five laboratories (Table 2). The relative abundance of the monogalactosylated / fucosylated species with *vs.* without bisecting *N*-acetylglucosamine (GlcNAc) ranged from 2.2 to 3.4 % in three laboratories (labs-1, 4 and 5), while others overestimated abundance or did not present the data due to insufficient separation of the oligosaccharides with or without bisecting GlcNAc.

MS of oligosaccharides

MS of oligosaccharides was carried out with MALDI or LC/ESI MS (Table 1). The former was employed by many laboratories, most of which derivatized by permethylation prior to analysis. Permethylation stabilizes the sialic acid residues by converting them to methyl esters, thus preventing sialic acid loss whilst also improving the efficiency of positive ion formation.

Transferrin

The results of sample A transferrin with attention to the sialylation of biantennary oligosaccharides and the minor glycans with triantennary branching or fucosylation are summarized in Figure 1a (labs 6-13, 15 and 16), and a typical MALDI time-of-flight (TOF) mass spectrum of permethylated oligosaccharides is shown in Figure 3. Standard deviations of the data provided by two laboratories, lab-12 (n=7) and lab-16 (n=2), were small especially for the combination of permethylation and MALDI MS (lab-12). The abundance of monosialylated species was 11.0 ± 5.1 % (mean ± SD) in seven laboratories using a combination of permethylation and MALDI MS, a little higher than the results obtained with chromatography (Figure 1b). Four laboratories had levels below 15% for the monosialylated chain, whereas the higher levels obtained by others (labs 10-12) were probably due to sialic acid loss during sample preparation. The (fully sialylated) triantennary oligosaccharide level ranged from 0 to 5.6 %, apparently lower than the chromatographic data, and two laboratories (labs-6 and 10) failed to detect this oligosaccharide. The fucosylated oligosaccharide in seven laboratories (labs 6-12) ranged from 0 to 9.2 %, comparable to the chromatographic results. One laboratory (lab-12) repeated the measurement for the same sample and reported good intra-assay CVs less than 5 % for either oligosaccharide. One laboratory applied pyridylaminated oligosaccharides to MALDI TOF MS, which showed significant sialic acid loss. LC/ESI MS was employed by two laboratories (labs-15 and 16), and the results were a little different each other with respect to the levels of monosialo and triantennary species. In most measurements employing MALDI MS or LC/ESI MS, the fucosylated species was more abundant than the triantennary branching species, consistent with the chromatographic data. In summary, the results from three different methods, which were carried out in different laboratories, were similar each other as shown in Figure 1b.

IgG

The results for sample B IgG are presented in Figure 2a (labs 5-8, 11-16) with attention to the galactosylation levels as well as the minor component, monogalactosylated biantennary oligosaccharide bearing bisecting GlcNAc. Galactosylation in this sample was evaluated according to the relative abundance of three major species as a percentage of the total. Repeated measurements were performed in labs-12 and 16. The CVs in lab-12 with permethylation and MALDI MS were quite small. The standard deviations of the

measurement by lab-16 were exceptionally large for this specific sample, but the CVs for these species were less than 10% for samples A and C in the same laboratory. With either MALDI or LC/ESI MS, the most abundant *N*-linked oligosaccharide from sample B IgG was the monogalactosylated species by both MALDI and LC/ESI MS. The galactosylation levels calculated from the MALDI MS measurements ranged from 0.80 to 1.10 (0.93 ± 0.10) mol per fucosylated biantennary oligosaccharide chain, but those calculated from LC/ESI MS measurements (1.10 and 1.29 mol) were slightly higher (Table 3). The relative levels of the monogalactosylated and fucosylated glycan bearing bisecting GlcNAc calculated by mass spectrometric measurements were over the range of 2.2 - 14.0 % of total oligosaccharides, which was comparable to that obtained by chromatography. Similarly to the transferrin study described above, the results on IgG oligosaccharides from three different methods were comparable each other (Figure 2b). Typical mass spectra of permethylated oligosaccharides are shown in Figure 4.

Reproducibility of MALDI MS quantitation of permethylated oligosaccharides

Reproducibility of MALDI MS quantitation was evaluated by a supplementary experiment carried out in one laboratory (lab-17), where sample B (0.3 mg) was divided into three portions and each sample was separately subjected to permethylation followed by MS.

The coefficients of variation (CVs) of the five repeated measurements, or intra-assay CV, were less than 10% (1.3 – 8.8% for three major oligosaccharide species and 12 - 34% for the minor one (Table 3). The inter-assay CV was 0.1 - 4.2% for major species and 13% for the minor one. In this experiment, the sensitivity for small components was approximately 0.4% of their proportion among total oligosaccharides, when defined by the detection of ions with a signal-to-noise ratio of more than 2.

MS of glycopeptides

Nine laboratories performed MS of glycopeptides, and seven presented qualitative data or quantitative results for a single sample. Two laboratories presented sufficient, as well as remarkable, data with LC/ESI MS/MS (lab-15) or MALDI TOF MS (lab-17).

First, the difference between the oligosaccharide profiles at the two glycosylation sites of transferrin was revealed as shown in Figure 5a, where the levels of fucosylation and triantennary branching of transferrin were higher for the oligosaccharide attached to Asn-630 than for that attached to Asn-432, and this site-specific oligosaccharide profile difference was quite consistent between the results from these two laboratories. As shown by the MALDI TOF mass spectra in Figures 5b and 5c, the heterogeneity of oligosaccharide structures was more obvious at Asn-630, while a very low level of fucosylation could be identified in the Asn-432 oligosaccharides by tandem MS of the ion observed at *m/z* 3830 (data not shown). In addition, the level of fucosylated biantennary oligosaccharide exceeded that of the triantennary oligosaccharide, consistent with the chromatographic or mass spectrometric

analyses of the released oligosaccharides. On the other hand, sialic acid loss was observed in the glycopeptide ions generated by MALDI. Good reproducibility was reported by lab-17 (Figure 5a).

Serum IgG is polyclonal and is thus a mixture composed of different primary protein structures. The amino acid sequence of the tryptic peptide involving the *N*-glycosylation site Asn-297 is heterogeneous; and EEQYNSTYR and EEQFNSTFT representing two subclass molecules, IgG1 and IgG2, respectively, are abundant. In this study, three IgG samples (A, B and C) from different individuals were analyzed. The relative abundances of subclass molecules were estimated as 1/3, 1/4 and 2/1 (IgG1/IgG2), for samples A, B and C, respectively, based on the total intensities of the corresponding groups of ions in the MALDI linear TOF mass spectra of enriched glycopeptides (Supplementary Figure 1). The amino acid sequences of these glycopeptide ions were verified by tandem MS in a separate experiment (data not shown). The galactosylation levels of IgG1 or IgG2 for each sample were calculated from the corresponding signals observed in the LC/ESI or MALDI mass spectrum (Supplementary Figure 2a) and summarized in Table 4. The results from these independent analyses were consistent; *i.e.* the agalacto species was more abundant than the digalactosylated species in the IgG2 from samples A and B, but not in the IgG1 from sample C. The oligosaccharides on the major subclass molecules, IgG2 for samples A or B, and IgG1 for sample C, should contribute more to the global glycan profiles of total IgG in each sample. The results from the MS of IgG glycopeptides were quite consistent with the chromatographic or mass spectrometric measurements of the corresponding released oligosaccharides (Supplementary Figure 2b). Hypogalactosylation of IgG2 relative to IgG1 is not a common finding among different individuals (unpublished observation by YW).

The levels of minor glycans with bisecting GlcNAc in the major IgG subclass molecules were comparable between LC/ESI MS and MALDI MS (data not shown). The numbers of oligosaccharide structures identified as constituting more than 1% of the total oligosaccharides from sample B IgG were compared by different methods. Fifteen structures were seen by lab-1 using chromatography, nine and fourteen by lab-7 and lab-8, respectively, analyzing permethylated oligosaccharides with MALDI MS, fifteen by LC/ESI MS of glycopeptides and ten by MALDI TOF MS of glycopeptides (Supplementary Figure 3), indicating glycopeptide analysis to be sufficiently sensitive to detect minor glycans on IgG. No significant amounts of glycopeptides derived from other regions of IgG were found in these samples.

DISCUSSION

Oligosaccharides

The chromatographic quantitation of the reductively aminated oligosaccharides showed a significant variance among laboratories, despite the fact that the method has been accepted as established. Whether or not labeling efficiency is uniform for different glycan structures

and/or different fluorescent aromatic amines remains unclear, but the variance seems to be attributable to the use of different reaction protocols, which can result in incomplete derivatization. In addition, the insufficient separation of specific glycans, *e.g.* those with or without bisecting GlcNAc, resulted in a considerable variation in the quantitation (Figure 2b), while the chromatographic method discriminates isomers, *e.g.* monogalacto species bearing a galactose at either antenna in IgG.

It is generally accepted that MS does not allow real quantitation for oligosaccharides unless stable isotope-labeled analogues are incorporated as internal standards. In this multi-institutional study analyzing the same transferrin and IgG glycoprotein samples, however, MS has yielded quite comparable results with chromatography in the (relative) quantitation of oligosaccharides (Figures 1b and 2b). For MALDI, especially, the in-source and post-source decay of glycans are so well-known that one suspects it would be too difficult to detect their intact structures. Parameters such as laser wavelength and power, extraction voltages, and "hot" or "cool" matrices directly influence the internal energy of generated ions and the resulting fragmentation (Harvey, 1999). Furthermore, the distribution of molecular species in complex glycan mixtures within the matrix spot on the target depending on sample preparation is also a critical point and sufficient "averaging" of laser shots is essential. However, there are publications describing good quantitation of oligosaccharides based on the signal intensities observed in the MALDI mass spectrum (Harvey, 1993; Garozzo *et al.*, 1994). Indeed, a comparative study of the signal intensities generated from a mixture of equimolar amounts of various *N*-linked glycans did not show any significant difference for compounds with molecular masses over about 1 kDa (Naven and Harvey, 1996). In the present study, although different MALDI TOF instruments were used, the analytical parameters, such as the type of laser (nitrogen that emits at 337 nm), the choice of matrix (2,5-dihydroxybenzoic acid, DHB), the type of ion species for permethylated oligosaccharide detection (sodium-adduct ions $[M+Na]^+$) and the mode of TOF analysis (reflectron), were the same among the laboratories and yielded consistent results. In MALDI MS, the ions generated by hundreds of laser shots, each of which produces one mass spectrum, are accumulated from different points of laser irradiation. The procedure makes the reproducibility excellent in the repeated measurements by lab-12 and in the supplemental experiment, and the inter-assay reproducibility in the same laboratory was also quite good (Table 2).

Regarding the determination of sialylation levels, the glycosidic linkage of sialic acid is susceptible to prompt (in-source) decay in the MALDI process, and the sialic acid-substituted oligosaccharides are likely to decompose in the flight tube in the TOF instrument as well. In addition, the number of sialic acids affects the relative ionization efficiencies (Sutton et al., 1994). Consequently, the signal intensity of underivatized sialylated oligosaccharides in the MALDI mass spectrum cannot be directly related to concentration as shown by the results obtained by lab-13 for oligosaccharides only derivatized at the reducing end by aminopyridine (Figure 1). Permethylation, which has been used for more than 40 years in order to modify

hydroxyl groups of sugars (Hakomori, 1964; Ciucanu and Kerek, 1984; Ciucanu and Cotello, 2003), methylates the carboxylic acid group of the sialic acid to produce a neutral sugar, whereupon esterified sialic acid loss is avoided and the ionization efficiency becomes equivalent to that of natively neutral oligosaccharides. In addition, this type of derivatization prevents salt formation which complicates the mass spectrum and impairs the signal-to-noise ratio for the individual molecular ion species. Furthermore, the lack of hydroxyl groups also prevents the cleavage of other glycosidic bonds (Lemoine *et al.*, 1996), making the permethylated oligosaccharides resistant to in-source fragmentation. In fact, the sialylation levels determined by MALDI MS after permethylation were acceptable, although a variance exists among laboratories as was the case for chromatography. A special setup of derivatization required a smaller amount of samples (5 μg glycoprotein) to meet the high sensitivity of MALDI MS for permethylated oligosaccharides (Kang *et al.*, 2005), while routine analysis used ~100 μg in this study.

The levels of triantennary oligosaccharides determined by MALDI MS were lower than those from chromatography, though not markedly. It is not possible to decide which value is the correct one, but the decreased triantennary structures seen by MS may be due to the increased mass of 810.4 Da of an additional antenna, making the detector response for the triantennary oligosaccharide ions at *m/z* 3602.8 weaker than that for the biantennary ions at *m/z* 2792.4, or there may be increased collision-induced dissociation (CID) of an enlarged cross-section of structure. The peak broadening effect due to isotopes is only 17% for this mass increase and thus does not produce a substantial error even when the quantitation is based on the peak height in the MALDI mass spectrum. On the other hand, core fucosylation, which occurs at the 6-position of the reducing terminal GlcNAc in the transferrin oligosaccharides, does not affect quantitation by MALDI MS (Naven and Harvey, 1996). It is worth noticing that the level of the triantennary oligosaccharide was lower than that of the fucosylated species in measurements with either MALDI MS or chromatography, indicating that MALDI MS is similar in its ability to detect minor glycans. Similarly, good relative quantitation by MALDI MS was confirmed by IgG analysis, as the monogalactosylated species was the most abundant and the calculated level of galactosylation was comparable to that obtained by chromatography.

ESI MS was employed by two laboratories, where oligosaccharide alditols were separated by graphitized carbon chromatography and introduced on-line to an ESI mass spectrometer operated in the negative ion mode (Karlsson *et al.*, 2004). The reproducibility of LC/ESI MS was acceptable from the data of lab-16. Regarding sialylated oligosaccharides, ESI is soft enough to detect the intact oligosaccharides with sialylation unless high nozzle-skimmer potential is applied, even when sialic acids are not derivatized. However, the charge of sialic acids affects the efficiency of negative ion formation, and thus the distribution of multiply-charged ions in the mass spectrum is different from that for neutral oligosaccharides, disturbing straightforward quantitation of sialic acid-substituted

oligosaccharides in the mass spectrum or ion chromatogram at the same time as neutral glycans. Nevertheless, LC/ESI MS results were comparable to those from MALDI MS or chromatography as shown in Figures 1b and 2b, except that an increased level of monosialylated oligosaccharides from the transferrin sample was reported by one laboratory, possibly due to sialic acid loss during sample preparation. A brief summary of the methods for oligosaccharide analysis including capillary electrophoresis-MS (Zamfir *et al.*, 2000) is presented in Table 5.

In this study, some laboratories also presented MS/MS spectra of permethylated or reductively aminated oligosaccharides. For example, the product ion mass spectra provided branching and linkage information (Supplementary Figure 4). This method is used for structure verification, qualitatively, and is not primarily directed toward quantitation. However, along with the establishment of the strategies for *de novo* carbohydrate sequencing by an algorithm incorporating the fragmentation database and informatics (Ashline *et al.*, 2005; Tang *et al.*, 2005), quantitation of oligosaccharide isomers will be realized in the near future.

Glycopeptides

Glycopeptide analysis allows identification of site-specific oligosaccharide structures which are essential to understanding the role of local oligosaccharide structures in protein folding and functions. However, it is conceivable that the analysis of glycopeptides is difficult as compared to that of unglycosylated peptides or oligosaccharides, since chemical properties differ between the glycan and peptide components. Moreover, each glycopeptide is often a minor constituent in the peptide mixtures after enzymatic digestion of glycoproteins because of the large number of glycoforms expressed by many proteins at each site. These problems may be overcome by employing LC/MS and selecting the glycopeptides in the chromatogram by detection of the CID-generated glycan-specific oxonium ions (Huddleston *et al.*, 1993). Alternatively, glycopeptide fraction can be enriched by lectin or other extraction tools, and the fraction can be directly analyzed by MS, especially when the glycoprotein has a small number of glycosylation sites, as is the case for transferrin and IgG (Wada *et al.*, 2004). The glycan and peptide structures of glycoproteins can then be elucidated by MS/MS of glycopeptide ions (Liu *et al.*, 1993; Krokhin *et al.*, 2004).

The MS of glycopeptides is usually performed in the positive ion mode to detect $[M+H]^+$ ions. In this case, protonation occurs on the peptide portion, and thus the signal intensity of the glycopeptide is largely dependent on the proton affinity of the peptide component of the molecule, thus rationalizing the quantitation of different glycoforms of a peptide according to their signal intensities. However, there are still a few concerns. Firstly, glycopeptides are larger than oligosaccharides and thus are accompanied by an increased risk of CID. Since the glycan moiety is more labile than the peptide backbone, the resulting cleavage of the glycosidic bonds may result in overestimation of the glycoforms with a smaller number of

building saccharides. This effect will be evident in the MALDI produced ions in which internal energies are higher than those of ESI ions. In previous reports, however, neutral oligosaccharides had minimal affect upon the ionization efficiencies of glycopeptides, and consequently, the integration of MALDI TOF signals of several desialylated glycopeptides yielded excellent quantitative correlations with published data obtained by established HPLC techniques (Sutton *et al.*, 1994; Harmon *et al.*, 1996). Secondly, the sialic acids of glycopeptides cannot be appropriately derivatized without deleterious modifications of the peptide component. In MALDI MS, the sialic acid loss occurs both in-source and post-source as described above, and occurs over a significant time frame in which a hydrogen transfers between suitably positioned functional groups (Harvey, 1999). Consequently, the sialic acid loss increases with the longer delay time before extraction (Naven *et al.*, 1997); and is prominent in the MALDI ion-trap type of mass separators. Most studies of sialylated glycopeptides with MALDI TOF MS are conducted in the linear mode so that the postsource decay ions are not separated. On the other hand, the sialic acid loss is minimal in ESI, but there are charge-dependent effects on the ionization efficiency and on the distribution of multiply-charged ions of the oligosaccharides.

Despite these problems, the site-specific analysis of glycoprotein oligosaccharides by MS is becoming popular. In the present study, the results from two laboratories on glycopeptides, one with MALDI MS and another with LC/MS, were consistent with each other, and were informative in terms of the oligosaccharide profiles specific to the protein sequence. The galactosylation levels at different polymorphic sequences of IgG explained well the global glycan profiles determined by the analyses of released oligosaccharides, and the oligosaccharide profiles of two glycosylation sites of transferrin were clearly shown to be different from each other. Although these findings could be obtained by isolation of each glycopeptide and subsequent analysis of released oligosaccharides, the direct analysis of glycopeptides performed herein is by far easier and more rapid as well as being sufficiently sensitive for minor glycans. The glycopeptide analysis requires a fairly small amount of samples (less than 10 μg glycoprotein in this study), and thus will contribute a great deal to the emerging field of glycoproteomics.

In conclusion, MALDI MS of permethylated oligosaccharides is as reliable as chromatographic methods for elucidating glycan profiles based on mass mapping of the compositional analysis. The publicly available murine and human MALDI MS glycomics data, which is being acquired by the Consortium for Functional Glycomics (www.functionalglycomics.org), for systems biology research are based on this approach. Good relative quantitation data can be achieved without neutralization of sialic acid residues by LC/ESI MS utilizing porous graphitized carbon as a separation medium for oligosaccharide alditols. Quantitative and relative quantitative datasets can be obtained by peptide sequencing and determination of glycosylation sites by LC-MS/MS of native